ЖУРНАЛ СТРУКТУРНОЙ ХИМИИ

2016. Том 57, № 1 *Январь – февраль* *С. 185 – 191*

UDC 541.67

EFFECTS OF A DONOR CONCENTRATION ON THE STRUCTURE OF Nb-DOPED NANO-SIZED $BaTiO_3$ POWDERS PREPARED BY MICROWAVE-HYDROTHERMAL SYNTHESIS METHODS

A. Khanfekr, M.Tamizifar, R. Naghizadeh

Department of Metallurgical and Materials Engineering, Iran University of Science and Technology, Narmak, Tehran, Iran
E-mail: khanfekr@iust.ac.ir

Revised December, 28, 2014

$BaTi_{1-x}Nb_xO_3$ compounds (with x = 0.00, 0.01, 0.03, 0.06, and 0.09) are synthesized by the microwave-hydrothermal (MH) method. The donor concentration effect on the structural properties is investigated. The new MH method is used instead of the previous solid state reaction for the $BaTiO_3$+Nb_2O_3 system. In the MH process, as the niobium incorporation rate increases, the particle growth substantially slows down. The synthesis of Nb-doped $BaTiO_3$ is investigated under the MH conditions subjected to 150 °C for only 2 h using $C_{16}H_{36}O_4Ti$ (tetra-n-butyl orthotitanate), $Ba(OH)_2 \cdot 8H_2O$, and $NbCl_5$ as Ba, Ti, and Nb sources respectively. For the phase evolution studies, X-ray diffraction patterns are analyzed and Raman spectroscopy is performed. The transmission electron microscope and the field emission scanning electron microscope images are taken for the detailed analysis of the grain size, surface, and morphology of the compound.

DOI: 10.15372/JSC20160122

K e y w o r d s: barium titanate, perovskites, niobium doping, chemical synthesis, microwave sintering, microstructure.

INTRODUCTION

Perovskite-type oxides have the general formula ABO_3, in which A is a rare earth or alkaline earth metal, B is a transition metal, and the oxides are typically *p*-type semiconductors. Their composition can be varied in a wide range by a partial substitution of a lower valent cation in A or B sites, yielding additional mobile anion vacancies. Their mixed conductivity by both ion and electron migration and their high nonstoichiometric composition have resulted based on the applications of this group of materials in the areas such as electrochemistry [1, 2], oxygen separation membranes [3], chemical sensors for the detection of humidity [4], alcohol [5], and gases such as oxygen [6], hydrocarbon [7] and nitric oxide [8] from three decades ago until the present time. As the result of a strong dependence of the ferroelectric properties on the grain size and compositional aspects, the microstructural control has become very important [9]. The doping of barium titanate (BT) ceramics by aliovalent dopants causes many changes in the properties of the materials such as conductivity, especially at high temperatures, morphology, dielectric behavior, and so on. The addition of donor dopants such as Nb at a relatively low concentration results in room-temperature semiconductivity with the positive temperature coefficient resistor (PTCR) behavior, whereas higher donor contents lead to insulating materials with a low concentration of oxygen vacancies and improved resistance to dielectric breakdown. The transition from the semiconductor behavior to the insulator behavior beyond a critical

donor concentration is due to a shift from the electron compensation to the cation vacancy compensation [10—12]. In the present paper regarding the solid state method, the results of studies with respect to processing Nb-doped $BaTiO_3$ are reported. Specifically, it is shown that Nb ions can be incorporated into the $BaTiO_3$ lattice in a narrow temperature range of 1523—1733 K. It is also shown that at temperatures lower than 1500 K Nb cannot be incorporated into the $BaTiO_3$ lattice due to the kinetic reason [12, 13].

Compared to the traditional solid state reaction and wet-chemical routes (including the sol-gel processing, oxalate route, and homogeneous precipitation), the hydrothermal method is low-cost and convenient to prepare $BaTiO_3$ nanoparticles without a subsequent high temperature calcination process [14—16]. In order to produce powders characterized by the desired size and shape, a variety of hydrothermal conditions has been investigated. These include the pH value, Ba/Ti ratio, reaction temperature as well as various precursors in the previous studies [17—19]. Although many efforts have been made to prepare $BaTiO_3$ particles, there is still little known about the effects of doping and solvent on the size and shape under hydrothermal conditions. A number of authors have synthesized $BaTiO_3$ by the MH method below 200 °C, however, the MH processing has not been reported by previous workers for different Nb-doped $BaTiO_3$. In this work, we investigated the effects of different concentrations of incorporating Nb on the properties of $BaTiO_3$; while a new MH method replaces the previous solid state reaction for the $BaTiO_3$+Nb_2O_3 system at a high temperature.

EXPERIMENTAL

The MH reactions were performed using a laboratory-made microwave-heating-autoclave system with a PTFE inner vessel and operating at a frequency of 2.45 GHz at 0—100 % of full power at 900W with a temperature control up to of 220 °C. An auxiliary cooling/heating device was fitted to the system, which enabled it to operate at a fixed temperature for a long time, while maintaining the input power of the microwave radiation during the reaction. $BaTi_{1-x}Nb_xO_3$ compounds (with x = 0.00, 0.01, 0.03, 0.06, and 0.09) were synthesized by the MH method. $C_{16}H_{36}O_4Ti$ (tetra-n-butyl orthotitanate), $Ba(OH)_2 \cdot 8H_2O$, and $NbCl_5$ reagents were used as raw materials. The starting materials were mixed at 70 °C in distilled water containing 1M NaOH to control the pH higher than 12 under stirring until it turned into a homogeneous solution [20]. The solution was transferred into a sealed autoclave and then filled with distilled water until the total volume reached 100 ml (80 % of the capacity of the autoclave).

The system was heat treated at 150 °C for 2 h. The resulting powders were centrifuged and washed with distilled water and finally oven dried at 85 °C for 24 h. The obtained powders were characterized by XRD (X′Pert PRO MPD) with CuK_α radiation in the 2θ range from 20° to 90° and Raman spectroscopy (BRUKER; spectral range 80—3500 cm^{-1}). The microstructural characterization was performed by field emission scanning electron microscope (FE-SEM) on MIRAII TESCAN and transmission electron microscopy (TEM) on PHILIPS-EM-208.

RESULTS AND DISCUSSION

Fig. 1 shows the XRD patterns of MH niobium doped barium titanate ($BaTi_{1-x}Nb_xO_3$) powders prepared at 150 °C for 2 h. The nanoparticles are pure perovskite Nb—$BaTiO_3$, without any intermediate carbonate phase that is usually observed with 2θ of 24° or 42° in the solid state method [16]. The presence of $BaCO_3$ can be attributed to the incomplete reaction, the presence of carbonate in the Ba alkali source, or to the reaction of CO_2 in the air. The crystallized Nb—$BaTiO_3$ sample is carbonate free, indicating that the MH technique was successful in producing pure crystalline nanoparticles [23].

The diffraction patterns at 2θ around 45° with a characteristic splitting of the (2 0 0) reflection for the tetragonal form in contrast to a symmetric peak for the cubic form and without a characteristic separation of the peak at 2θ of 45°, which correspond to the tetragonal structure, have been measured. An eventual tetragonal peak splitting of the reflections cannot be resolved due to the overlap on the (0 0 2) and (2 0 0) planes. However, the XRD peaks of the nanoparticles are broader than the larger

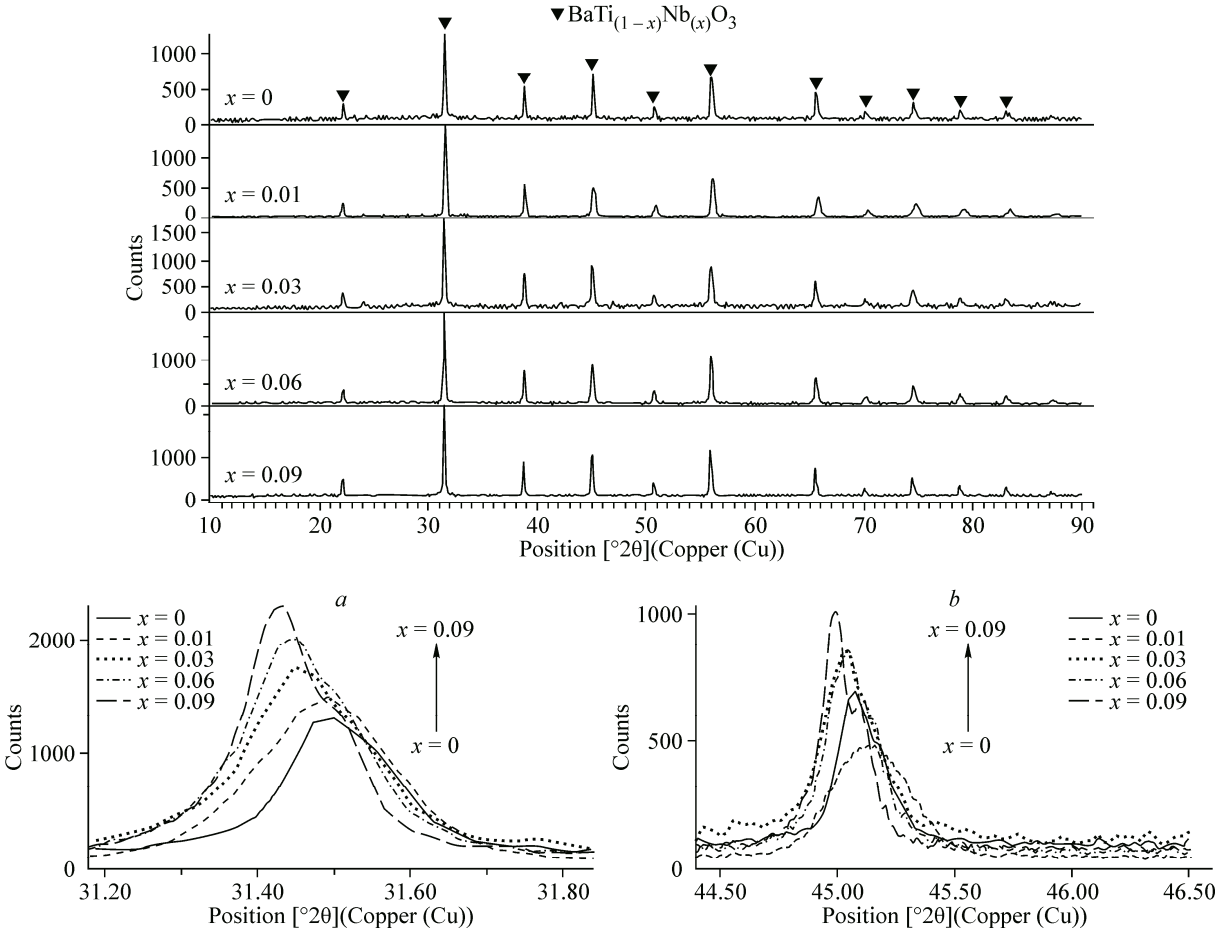

Fig. 1. XRD patterns of $BaTi_{1-x}Nb_xO_3$ nanoparticles with different magnifications (*a*), shows 2θ of 24° (*b*), is the (110) planes (*c*), and represents the (200) planes (*d*)

one, thus the cubic structure cannot be totally excluded, which often makes this splitting difficult for the determination [17, 21].

It is clearly seen that with the enhancement of niobium, the maximum peak shifts towards lower 2θ values as the intensity of the peaks increases. The result was in close agreement with the changes in the tetragonality. It was deduced that Nb^{5+} could substitute for Ti^{4+} in the $BaTiO_3$ lattice because the small ionic radius of Nb^{5+} (0.064 nm) is close to that of Ti^{4+} (0.061 nm). It has been reported that the Ti^{4+} substitution for Nb^{5+} decreased the tetragonality of $BaTiO_3$ ceramics [22, 23].

In order to investigate and relate these factors, the William-Hall and Scherrer methods were applied. The crystallite size of the powder was calculated using the Scherrer equation [24]

$$D_v = \frac{K\lambda}{B_{size}\cos\theta}, \tag{1}$$

where D_v represents the crystallite size; K is a constant with a value of 0.9; λ is the X-ray wavelength and the width if peak B_{size} was determined as the full width at half-maximum (FWHM). The resulted internal strain ε was calculated using the Williamson—Hall equation [25—28]

$$B_{size+strain}\cos\theta = \frac{K\lambda}{D_v\cos\theta} + 4\varepsilon\sin\theta. \tag{2}$$

For the samples of $BaTi_{1-x}Nb_xO_3$ compounds (with $x = 0.0$, 0.03, 0.06) Fig. 2 shows the graph of $B_{size+strain}\cos\theta$ against $4\sin\theta$ plotted from Eq. 2, and the internal strain is then obtained from the slope of the graph. Table 1 gives the results of the calculations of the internal strain and an average size of

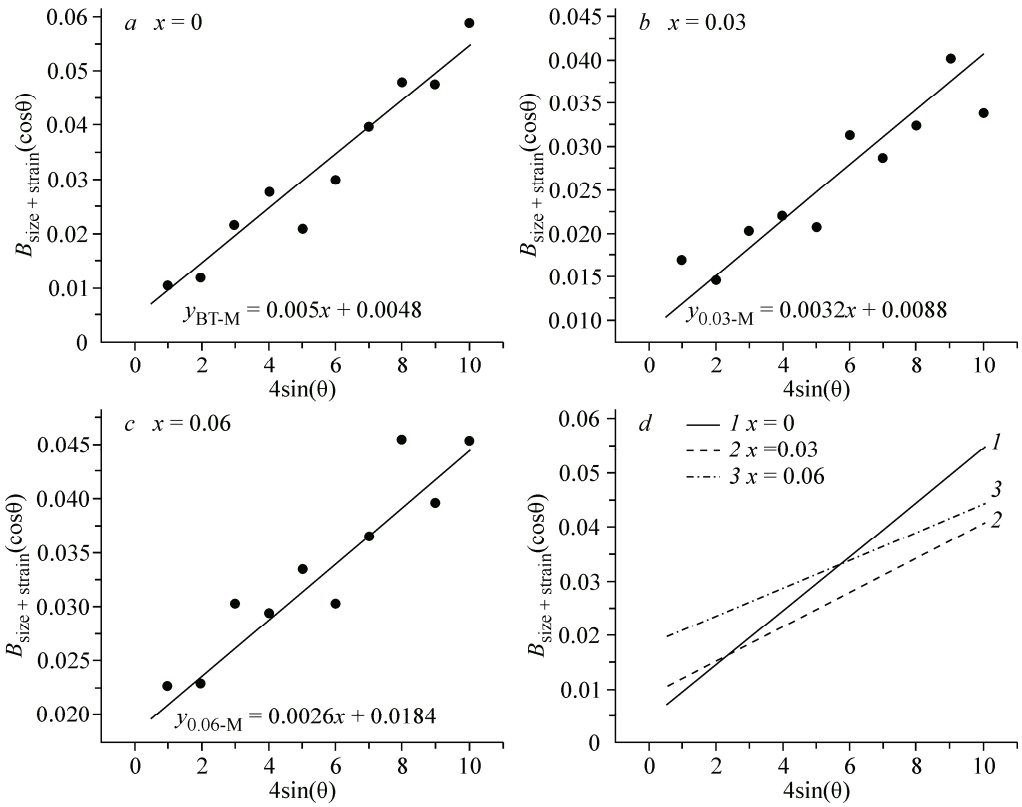

Fig. 2. Plot of $B_{size+strain}\cos\theta$ vs $4\sin\theta$ for: $x = 0.0$ (*a*), $x = 0.03$ (*b*), $x = 0.06$ (*c*), all-encompassing graph (*d*)

crystallites estimated from the broadening of the diffraction peak using the Scherrer and Williamson—Hall equations.

According to the results, the optimization of the crystal geometry of $BaTiO_3$ in the tetragonal phase after doping with Nb is attained by the impurity-outward displacements of barium. The movements are mainly in the *ab* plane while the motion along the *c* axis is practically negligible. The ratio of the *c* and *a* lattice parameters decreases with a Nb concentration and finally the transition of the $BaTiO_3$ crystalline phase from tetragonal to cubic occurs. Therefore the Ti^{4+} substitution for Nb^{5+} with a larger ionic radius decreases the tetragonality but increases the crystallite size and internal strain.

The calculated *a* and *c* parameters, and their ratios are shown in Table 1. The *a* and *c* lattice parameters increase with the Nb content, but the *a* lattice parameter increases more rapidly than *c*. According to the results, in the tetragonal phase the optimization of the crystal geometry of $BaTiO_3$ after doping with Nb is attained by the impurity-outward displacements of barium. The movements are

T a b l e 1

Crystallite size (nm), *microstrain* (ε), *and a and c lattice parameters of the powder calculated by the Scherrer and Williamson-Hall equations*

Sample	$x = 0.00$	$x = 0.03$	$x = 0.06$
Crystallite size (nm) — Scherrer	34.14	53.31	65.48
Crystallite size (nm) — Williamson-Hall	30.81	48.12	59.23
Microstrain (ε) — Williamson-Hall	0.0012	0.0022	0.0046
Lattice parameter *a* (Å)	4.0177	4.0253	4.0281
Lattice parameter *c* (Å)	4.0278	4.0283	4.0286

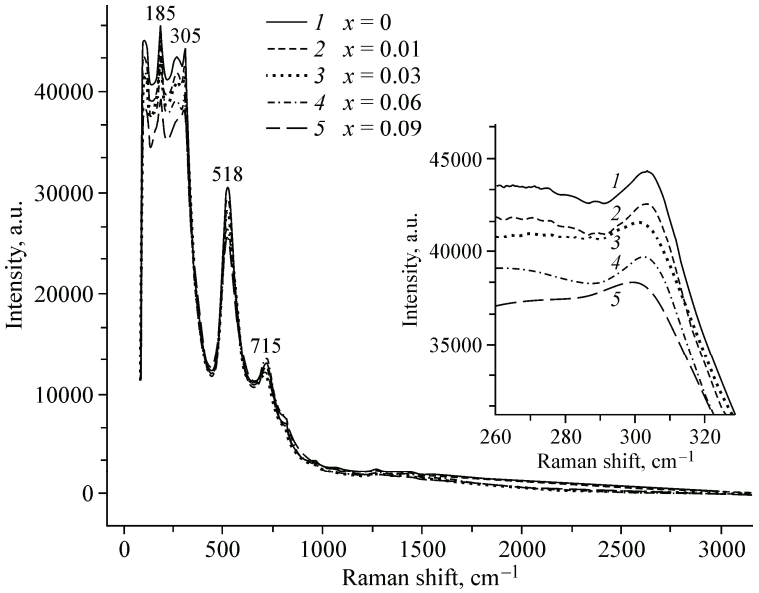

Fig. 3. Raman spectra of hydrothermal nanosized Nb—$BaTiO_3$ powders

mainly in the *ab* plane while the motion along the *c* axis is practically negligible. The ratio of *c* and *a* lattice parameters decreases with the Nb concentration.

Based on Raman studies, the particles are tetragonal rather than cubic due to the asymmetry of TiO_6 octahedra. The Raman spectra for the obtained Nb—$BaTiO_3$ ceramic powder samples obtained are presented in Fig. 3. The peaks at 185 cm^{-1} and 518 cm^{-1} are assigned to the TO mode of the A_1 symmetry and the sharp peak at 305 cm^{-1} is attributed to the B_1 mode, which are the characteristics of tetragonal $BaTiO_3$. The weak peak at 715 cm^{-1} is assigned to the highest-frequency longitudinal optical (LO) mode with the A_1 symmetry characteristic of tetragonal $BaTiO_3$ as well [29—31].

The FE-SEM images of the prepared $BaTi_{1-x}Nb_xO_3$ compounds (with x = 0.3, 0.06) are shown in Figs. 4 and 5 respectively. In the MH process, microwave radiation can couple with and be absorbed by the dielectric material, and thus, smaller $BaTiO_3$ particles dissolve more quickly. According to the

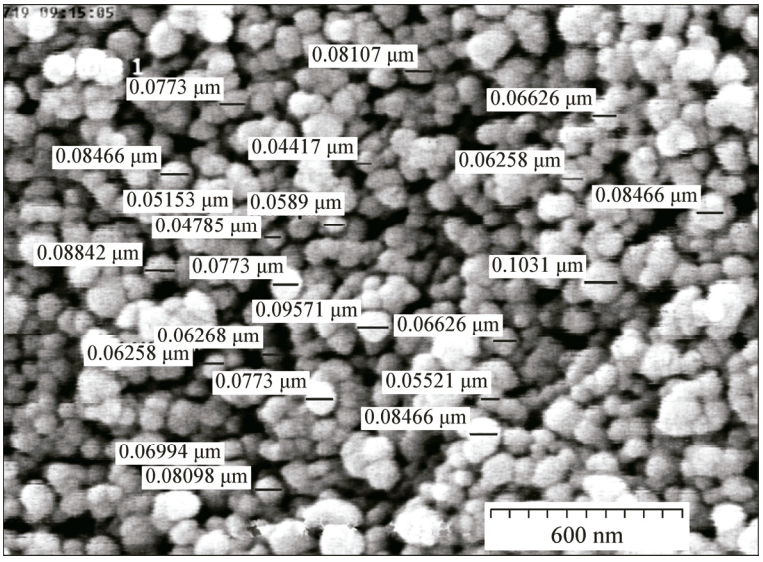

Fig. 4. $BaTi_{1-x}Nb_xO_3$ (x = 0.03) powders prepared at 150 °C for 2 h

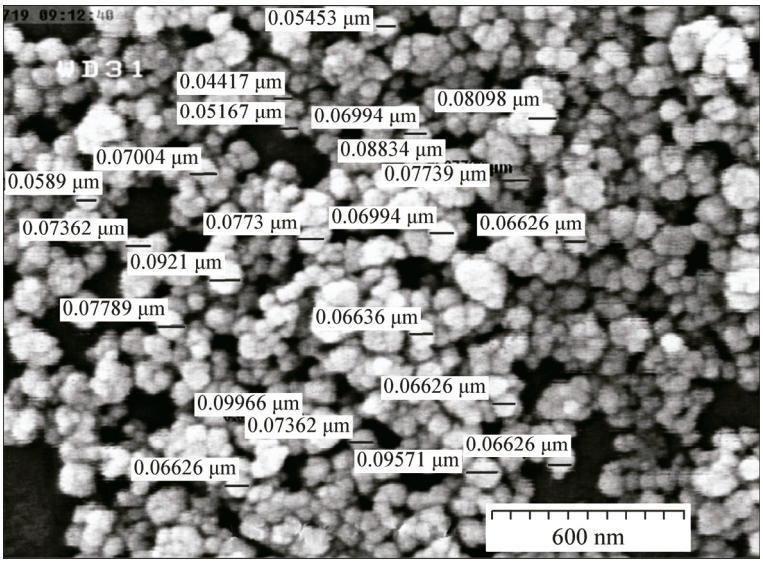

Fig. 5. $BaTi_{1-x}Nb_xO_3$ (x = 0.06) powders prepared at 150 °C for 2 h

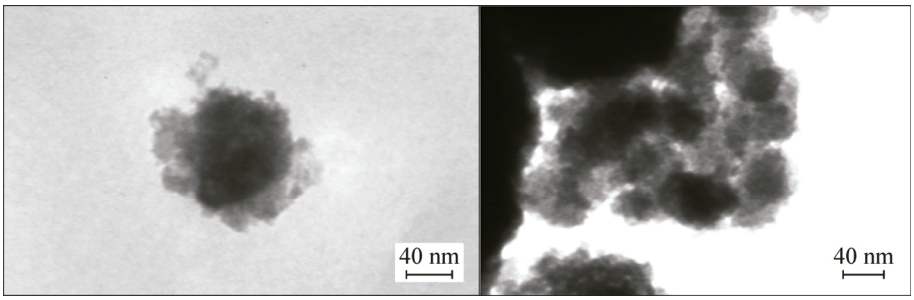

Fig. 6. TEM image of the Nb—$BaTiO_3$ (Nb = 0.01) powders

dissolution/recrystallization mechanism, this also causes a more rapid growth of larger particles [19, 32, 33]. The Ti^{4+} substitution for Nb^{5+} with a larger ionic radius increases the crystallite size.

It shows that the samples of the $BaTi_{1-x}Nb_xO_3$ powder, where x = 0.03 and 0.06, prepared for 2 h consist of ultrafine, well dispersed particles with the spherical morphology and the average particle size of 75 nm and 95 nm respectively.

Moreover, the TEM images of the sample of $BaTi_{1-x}Nb_xO_3$ compounds with x = 0.01 were taken in order to estimate the particle size and morphology. They are shown in Fig. 6. Most particles are spherically shaped crystals with an average size of 65 nm and this result is in good agreement with the XRD and SEM data. The decreased crystallite size in the MH method might be related to the increased nucleation rate and the high energy which activate chemical reactions at low temperatures. The nucleation rate should be high because of a high heating rate in the MH processes and the Ti^{4+} substitution for Nb^{5+} with a larger ionic radius increases the crystallite size.

CONCLUSIONS

The present investigation shows that Nb—$BaTiO_3$ powders with nanosized particles can be obtained by the rapid and cost-effective microwave-assisted hydrothermal process without a temperature gradient and uneven nucleation and growth of particles of various sizes. The MH method can be very fast and uniform, through a self-heating process arising from the direct absorption of microwave energy into the reaction mixture. This rapid homogeneous heating, not possible by convectional heating, provides the uniform nucleation, owing to which uniform-sized particles can be prepared.

The nanoparticles were pure perovskite Nb—$BaTiO_3$, without some intermediate carbonate phase that was usually observed in the solid state method. It was deduced that Ti^{4+} could substitute for Nb^{5+} in the $BaTiO_3$ lattice and the Ti^{4+}substitution for Nb^{5+} with a larger ionic radius decreased the tetragonality but increased the crystallite size and internal strain.

REFERENCES

1. *Kharton V.V., Yaremchenko A.A., Naumovich E.N.* // J. Solid State Electr. – 2000. – **3**, N 6. – P. 303 – 326.
2. *Bi Z., Cheng M., Dong Y., Wu H., She Y., Yi B.* // Solid State Ionics. – 2005. – **176**, N 7-8. – P. 655 – 661.
3. *Takamura H., Enomoto K., Aizumi Y., Kamegawa A., Okada M.* // Solid State Ionics. – 2004. – **175**, N 1-4. – P. 379.
4. *Holc J., Slunečko J., Hrovat M.* // Sensors Actuat. B-Chem. – 1995. – **26**, N 1-3. – P. 99 – 102.
5. *Kong L.B., Shen Y.S.* // Sensors Actuat. B-Chem. – 1996. – **30**, N 3. – P. 217 – 221.
6. *Lukaszewicz J.P., Miura N., Yamazoe N.* // Sensors Actuat. B-Chem. – 1990. – **1**, N 1-6. – P. 195 – 198.
7. *Brosha E.L., Mukundan R., Brown D.R., Garzon F.H., Visser J.H., Zanini M., Zhou Z., Logothetis E.M.* // Sensors Actuat. B-Chem. – 2000. – **69**, N 1. – P. 171 – 182.
8. *Traversa E., Matsushima S., Okada G., Sadaoka Y., Sakai Y. Watanabe.* // Sensors Actuat. B-Chem. – 1995. – **25**, N 1. – P. 661 – 664.
9. *Vijatović M.M., Bobić J.D., Stojanović B.D.* // Science of Sintering. – 2008. – **40**. – P. 155 – 165.
10. *V'yunov O.I., Kovalenko, Belous A.G.* // Inorg. Mat. – 2006. – **42**, N 12. – P. 1363 – 1368.
11. *Stojanovic B.D., Foschini C.R., Zaghete M.A., Veira F.O.S., Peron K.A., Cilense M., Varela J.A.* // J. Mater. Proces. Technol. – 2003. – **143-144**. – P. 802 – 806.
12. *Nowotny J., Rakas M.* // Ceramics International. – 1994. – **20**. – P. 265 – 275.
13. *Brzozowski E., Castro M.S.* // J. Mater. Proces. Technol. – 2005. – **168**. – P. 464 – 470.
14. *Yuan Y., Zhang S.R., Zhou X.H., Tang B.* // J. Mater. Sci. – 2009. – **44**. – P. 3751 – 3757.
15. *Liu L., Guo H., Lü H., Dai S., Cheng B., Chen Z.* // J. Appl. Phys. – 2005. – **97**. – P. 054102.
16. *Brzozowski E., Castro M.S., Foschini C.R., Stojanovic B.* // Ceramics International. – 2002. – **28**. – P. 773 – 777.
17. *Chen C., Wei Y., Jiao X., Chen D.* // Mater. Chem. Phys. – 2008. – **110**. – P. 186 – 191.
18. *Xu H., Gao L.* // Mater. Lett. – 2004. – **58**. – P. 1582 – 1586.
19. *Sun W., Li C., Li J., Liu W.* // Mater. Chem. Phys. – 2006. – **97**. – P. 481 – 487.
20. *Yaseen H., Baltianski S., Tsur Y.* // J. Am. Ceramic Society. – 2006. – **89**, N 5. – P. 1584 – 1589.
21. *Noh H.-J., Lee S.-G.* // Transactions on electrical and electronic materials. – 2009. – **10**, N 2. – P. 121 – 125.
22. *Liu L., Guo H., Lü H., Dai S., Cheng B., Chen Z.* // J. Appl. Phys. – 2005. – **97**. – P. 054102.
23. *Szymczak L., Ujma Z., Adamczyk M., Pawełczyk M.* // Ceramics International. – 2008. – **34**. – P. 1993 – 2000.
24. *Newalkar B.L., Komarneni S., Katsuki H.* // Mater. Res. Bull. – 2001. – **36**. – P. 2347 – 2355.
25. *Mote V.D., Purushotham Y., Dole B.N., Mote et al.* // J. Theoret. Appl. Phys. – 2012. – **6**. – P. 6.
26. *Purushotham E., Krishna N.G.* // Bulletin of Materials Science. – 2009.
27. *Herrmann M., Engel W., Giibel H.* // JCPDS-International Centre for Diffraction, Advances in X-ray Analysis. – 2002. – **45**. – P. 212 – 217.
28. *Weier M.* // J. Chem. Engineering. – California university, 2005.
29. *A'vila H.A., Ramajo L.A., Reboredo M.M., Castro M.S., Parra R.* // Ceramics International. – 2011.
30. *Min B., Moon S.-M., Cho N.-H.* // Current Appl. Phys. – 2011. – P. 1 – 4.
31. *Lazarevi Z., Cevi N.R., Vijatovi M., Paunovi N., Cevi M.R., Stojanovi B., Cevi-Mitrovi Z.D.* // Acta Phys. Polonica A. – 2009. – **115**, N 4.
32. *Jhung S.H., Lee J.-H., Yoon J.W., Hwang Y.K., Hwang J.-S., Park S.-E., Chang J.-S.* // Mater. Lett. – 2004. – **58**. – P. 3161 – 3165.
33. *Hotta Y., Tsunekawa K., Duran C., Sato K., Nagaoka T., Watari K.* // Mater. Sci. Engineering A. – 2008. – **475**. – P. 57 – 61.